

Optimisation of temperature for growth of tin oxide on Ag(111)

Suvankar Chakraborty

Applied science department, Haldia Institute of Technology, Haldia, India

ABSTRACT

To find the right temperature to grow the tin oxide film, Sn-Ag alloy was formed by evaporating Sn on to Ag(111) surface and oxidised at to form tin oxide films . 3 ML Sn was deposited on to the silver surface and oxidised at 250° C and 300° C. Low energy electron diffraction (LEED) and angle resolved photoemission spectroscopy (ARPES) study was done to confirm the appropriate temperature. $(\sqrt{3} \times \sqrt{3})R30^\circ$ LEED pattern confirms the presence of Sn-Ag alloy phase at 250° C which disappeared due to formation of oxide phase at 300° C. Presence of surface bands, signature of alloy phase was observed for 250° C grown sample which was not present and appearance of new band due to oxide phase was observed with ARPES for 300° C grown sample.

Keywords –ARPES, LEED, Thin Film growth

I. INTRODUCTION

Most of the metallic surface in reality is covered with oxide surface due to the oxidation of the metal and it is this oxide layer that mostly govern the surface structure, reactivity and electronic structures for those material. Oxide has vast application too from paint pigment, non-linear optics, microelectronics, data storage sensors and catalysis etc. [1,2]. With the advancement in thin film growth technique studies of oxides surfaces are on the rise as wider range of oxides can be grown on different metallic substrates by molecular beam epitaxy method (MBE). On the other hand, 2D atomically thin metals, semiconductor and surface alloys show Rashba effect and topological insulator behaviour. Rashba effect was reported for reconstruction on Ag(111) substrate by Bi, Pb, Sb [3,4,5]. This was also the main motivation behind the study for Sn/Ag(111). In these cases, it was found that every third silver atoms are replaced by the deposited metal atom forming $(\sqrt{3} \times \sqrt{3})R30^\circ$ pattern. People have mostly oxidized this 1/3rd layer of Sn to form the oxide, but there is a lack of study available for higher thickness. Tin oxide, on the other hand can be used as a solid-state gas sensor material, oxidation catalyst, and transparent conductor [6, 7] anode material in Li rechargeable batteries, catalyst for several acids, precursor for thin transparent tin dioxide film electrodes, coating materials etc. [8].

Our motivation for the current study is to find the best condition to grow tin oxide by oxidizing the Sn-Ag(111) surface layer for moderate to higher thickness. We have already studied growth of tin oxide on Ag(001) [9] by co-deposition of Sn in oxygen atmosphere where we have grown 1 monolayer equivalent (MLE), 2MLE... and so on, up to 10 ML thickness. In this paper, I have tried to see directly growing moderate thickness (3MLE) tin film directly and then anneal that in oxygen atmosphere. Our main interest was to see is there any interface effect coming into play i.e., if we grow 3ML directly rather than growing 2 MLE on top of 1 MLE. We annealed the same at 250° C and 300° C and studied the sample using low energy electron diffraction (LEED) and angle resolved photoemission spectroscopy (ARPES).

II. OXIDES OF TIN: STANNOUS OXIDE (SnO) AND STANNIC OXIDE (SnO₂)

There are two main oxides of tin: stannous oxide (SnO) and stannic oxide (SnO₂). SnO and SnO₂ have litharge (α -PbO) and rutile structure as shown in Fig. 1 generated by VESTA software. SnO has a tetragonal structure (tP4, P4/nmm, SG No. 129, Z=2) with $a = b = 3.80295 \text{ \AA}$, $c = 4.83828 \text{ \AA}$, $c/a = 1.27$ [10,11]. Oxygen atoms occupy Wyckoff 2c sites at (0,0,0) and (1/2,1/2,0) and Sn atoms occupy Wyckoff 2a sites at (0, 1/2, u) and (1/2, 0, -u) with $u = 0.2369$ [10,12]. The structure of SnO is made of layers and each Sn atom is at the apex of a square pyramid whose base is formed by four oxygen atoms. All Sn-oxygen nearest neighbor (ONN) distances are equal to 2.22 Å. Each oxygen ion is surrounded by four Sn ions. SnO₂, on the other hand crystallizes in tetragonal rutile-type (tP6, P42/mnm, SG No. 136, Z=2) with $a = b = 4.7374 \text{ \AA}$, $c = 3.1864 \text{ \AA}$, $c/a = 0.672$ [13,14]. The structure is described as oxygen atoms at (v, v, 0; 1/2 + v, 1/2 - v, 1/2) and Sn atoms at (0, 0, 0) and (1/2, 1/2, 1/2) with $v = 0.30561$ [13] or

0.30644[14]. u and v are the dimensionless internal parameters representing the distance between Sn plane and its nearest neighbor O plane for each structure, respectively.

Stannous oxide is less characterized than SnO_2 as there have been controversies surrounding SnO. Different phase diagram of Sn-O was reported[15,16]but they do not agree with each other. No single crystal of SnO is available to characterise it in details. The stability of SnO is also not well established. It has been reported that SnO is stable at temperature range from 198 K to 543 K[15]. Some group did not even show SnO in their equilibrium phase diagram[16].Intermediate compounds of tin oxides such as, Sn_2O_3 , Sn_3O_4 and Sn_5O_6 are still debatable [17,18,19].Moreover, the electronic band gap of SnO is not accurately known but reportedly lies in the range of 2.5-3eV whereas experimentally the band gap is found to be 0.7eV [20,21].

Compared to SnO_2 , SnO has not attracted much interest among the researchers. One of the main reasons for this is that SnO undergoes rapid oxidation to form SnO_2 upon heating [22]. The heat of formation for SnO_2 and SnO at 298 K were found to be $\Delta H = -138\sim\text{cal/mol}$ and $\Delta H = -68\sim\text{cal/mol}$ resulting in $\Delta H = -70\sim\text{cal/mol}$ for the reaction $\text{SnO}(c) + 1/2 \text{O}_2(g) \rightarrow \text{SnO}_2(c)$ [20]. This indicates that the stannic oxide is the thermodynamically most stable form among tin oxides. On the other hand, above 1500°C , SnO_2 can be decomposed into SnO, a reduced form of Sn_2 and O_2 [20]i.e. SnO exist on the surfaces of SnO_2 . So, it is interesting to study the surface of tin oxides. However, discrimination between SnO and SnO_2 is difficult due to the very small shift of Sn3d core level binding energy. Using electron spectroscopy for chemical analysis, Lau and Wertheim [23]concluded that SnO and SnO_2 have negligible chemical shift between them as change in the free ion potential of Sn^{4+} and Sn^{2+} is cancelled by the Madelung potential at tin sites in SnO and SnO_2 and to distinguish them one needs to compare their valence bands and O/Sn ratio. However, a shift of 1eV in binding energy was also reported for transformation of SnO_2 to SnO [24]. In another report [25],it was shown that a shift of 0.7 eV occurs between Sn3d core level with a binding energy difference of 1.6 eV between SnO and SnO_2 . Most prominent way to distinguish the two oxides is to study their valence band. Unlike SnO_2 , Sn5s state is not empty for SnO as Sn5s does not take part in bonding and contribute to the valence band.

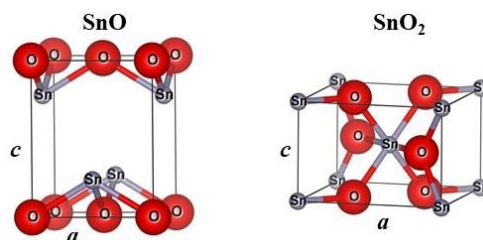


Figure. 1. Structures of litharge SnO and rutile SnO_2 generated by VESTA. Both SnO and SnO_2 show tetragonal symmetry

III. EXPERIMENTAL STUDY

Alloy structures of metallic tin (Sn) on silver surfaces were already studied and reported by us [26,27,28]. Growth of tin oxide on Ag(001) substrate were also reported [9]. In case of Ag(001) and Ag(111) the metallic tin form different alloys due to the different surface structure of the substrate. Similar tendency may occur for oxide formation. Tin oxide can be grown on any substrate by mainly two process – either by oxidation of the metallic tin alloy film or co-deposition of metallic Sn in oxygen atmosphere. There are lots of unanswered question- whether both the oxide film will give similar surface and electronic structure or not. As there is very little information was available in literature, main intention initially was to find and fix the optimum condition to find the better temperature for oxidation. It was already known that the oxidation at room temperature mostly gives metallic Sn giving very small amount of tin oxide films[9]. So, the reactive deposition or the oxidation has to be done at higher temperature. Sn alloy with silver were reported at 200°C [29].So, we decided to study the formation of tin oxide at 250°C and 300°C . The temperature was not raised further so that silver and tin metal does not starts to melt. 1 ML in case of metallic Snis defined as the thickness of the Sn layer having same surface atomic density asthat of the substrate. For oxides of tin, it is assumed that 1 ML Sn is oxidised togive one monolayer equivalent (MLE) oxide layer.

Tin alloy with Ag(111) was grown at 200°C . The alloy then oxidized by annealing at 250°C and 300°C by keeping the substrate at the same temperature in oxygen atmosphere. Oxygen was leaked into the chamber through a needle valve at pressure 6.5×10^{-6} mbar. A capillary was connected to the valve inside the chamber so that oxygen can be put as close to the substrate surface. Initially, a well-ordered Ag(111) single crystal substrate was prepared by repeated cycles of Ar^+ ion sputtering (600eV, $1\mu\text{A}$) for 15min, followed by annealing to 550°C for 30 min, until a

sharp $p(1 \times 1)$ LEED pattern was observed. Cleanliness of the substrate was also confirmed with XPS measurements where no impurity peaks were detected. High purity Sn (99.999%) was evaporated in the preparation chamber from a homemade resistive-type evaporator. The rate of deposition was maintained at $0.2 \text{ \AA}/\text{min}$, calibrated using a water-cooled quartz crystal thickness monitor mounted on a linear drive which was moved to the sample position for rate measurements prior to deposition. A MLE is defined as atomic density of $1.38 \times 10^{19} \text{ atoms}/\text{m}^2$, corresponding to that of the Ag(111) surface, would form the oxide film after oxidation. LEED measurements were performed at RT using a four-grid LEED apparatus (OCI Vacuum Microengineering) coupled with a highly-sensitive 12-bit CCD camera, to determine the crystalline quality of the deposited film, as well as the crystallographic symmetry directions. XPS measurements were performed in the analysis chamber with base pressure better than $8 \times 10^{-11} \text{ mbar}$ and attached to the preparation chamber. Photoemission measurements were performed using a combination of VG SCIENTA-R4000WAL electron energy analyzer with a 2D-CCD detector which has been described in detail elsewhere[30].

IV. RESULT AND DISCUSSION

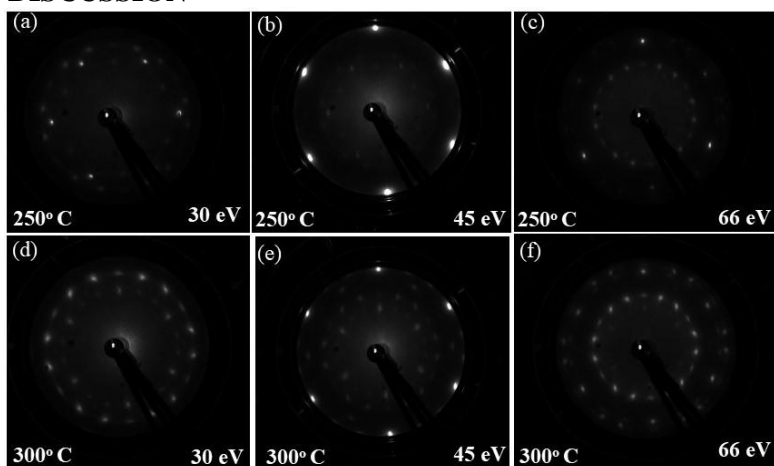


Figure. 2. LEED pattern for grown films at 250° C [(a)-(c)] and 300° C [(d)-(f)] at different electron primary beam energy

In previous tin oxide study by us [9], in order to achieve layer-by-layer growth, tin oxide was formed for one monolayer and continued up to 10 monolayer equivalents. After deposition of each monolayer the experimental data was taken. Here instead of growing one layer at a time we wanted to oxidized the alloy to form tin oxide and check is there any similarity. To do so, we have chosen a moderate thickness of Sn films. We have deposited 3 ML of Sn on Ag(111) to form tin-silver alloy. The alloy was then annealed at 250° C and 300° C respectively in oxygen environment and the data was taken at room temperature. The surface crystalline structure was studied using the LEED. In Fig. 2, the LEED pattern for the grown oxidized film is shown for both 250° C (Fig. 2 (a)-(c)) and 300° C (Fig. 2 (d)-(f)). With the increase in energy of the electron beam the field of view increases and clear LEED pattern is visible. For 250° C annealed oxide film, the LEED pattern is not clear, sharp $p(1 \times 1)$ spots for Ag(111) is visible in addition to the $(\sqrt{3} \times \sqrt{3})R30^\circ$ pattern for Sn-Ag alloy for 45 eV. At 66 eV, the faint LEED spots corresponding to tin oxide in visible for first case. For 300° C grown sample the LEED pattern at 30 eV clearly shows the pattern corresponding to tin oxide which was not visible at this electron beam energy for 250° C grown sample. $p(1 \times 1)$ spots for Ag(111) is also more sharp in case of later (see Fig. 2(e)). At 66 eV, it is clear from the image that the sample grown at 300° C has much more spots and better oxidized than the one grown at 250° C where the spots are diffused may be due to the presence of diffused oxygen at the surface.

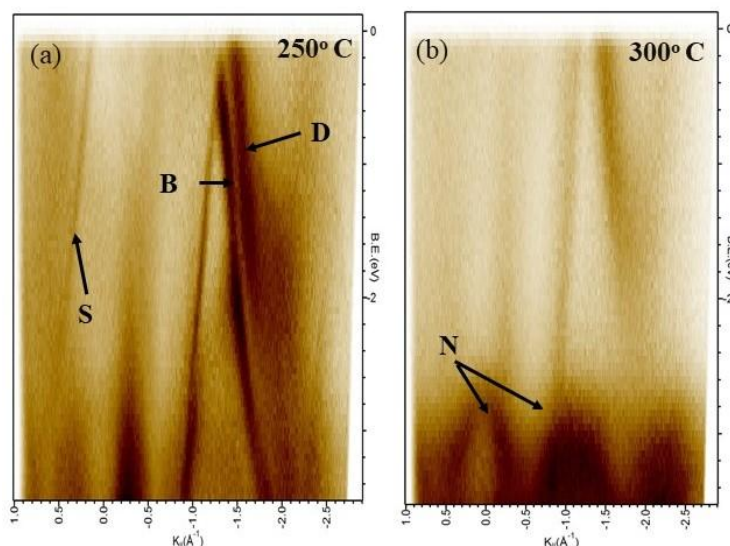


Figure. 3. Band dispersion of the grown film at (a) 250° C and (b) 300° C in $\bar{\Gamma}$ - \bar{M} direction. See text for details

To confirm the findings of the LEED pattern, we have also studied the electronic structure by ARPES method. The band structure of the both films were studied by ARPES using He II_α (40.8 eV) along $\bar{\Gamma}$ - \bar{K} direction and $\bar{\Gamma}$ - \bar{M} direction. The symmetry direction of Ag(111) is taken as the symmetry direction for the film as the exact phase of the grown film is not known. The symmetry direction is chosen as the symmetry direction of the Ag(111) SBZ. The energy range shown in the figure is limited to 3.5 eV below the Fermi energy (E_F) to avoid intense emission from the Ag 4d bands. For 250° C grown sample in $\bar{\Gamma}$ - \bar{M} direction, surface band S with $(\sqrt{3} \times \sqrt{3})R30^\circ$ periodicity, signature of Sn-Ag surface alloy is seen [see Fig. 3 (a)] near $\bar{\Gamma}$ point. In addition to that, a weak dispersive feature D can be seen around \bar{M} point. Ag bulk band, labelled B, can also be noticed. All these bands are mostly features of Sn-Ag alloy which prove that at 250° C the features of Sn-Ag alloy are mostly present and they are not fully oxidized. For 300° C grown sample in $\bar{\Gamma}$ - \bar{M} direction, most of the bands like surface band S is absent. Only faint features of bulk band are seen with an opening at Fermi energy which was not present in previous case. The appearance of new band with parabolic dispersion N for the 300° C sample is due to the oxide phase present in film. The absence of sharp band feature confirms that the oxide phase is not properly ordered. Similar features can also be seen for the 250° C grown sample in $\bar{\Gamma}$ - \bar{K} direction [see Fig. 4 (a)]. Here also the presence of surface state band S, bulk band B and diffused band D can be seen. The disappearance of all these bands at 300° C confirms that the Sn-Ag surface alloy is getting converted to oxide layer. The appearance of the new band N and gap opening at Fermi level near \bar{K} point confirm the formation of oxide phase.

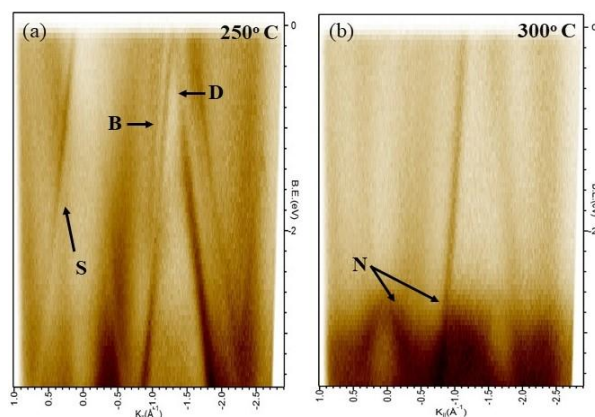


Figure. 4. Band dispersion of the grown film at (a) 250° C and (b) 300° C in $\bar{\Gamma}$ - \bar{K} direction. See text for details

V. CONCLUSION

To summarise, Sn was evaporated on to Ag (111) to form Sn-Ag alloy. 3 ML Sn was deposited on silver for that purpose. 3 ML Sn/Ag(111) alloy film then oxidized at 250° C and 300° C to check which one forms better oxide films. For 250° C grown sample ($\sqrt{3} \times \sqrt{3}$)R30° LEED pattern was noticed which confirms the Sn-Ag alloy phase. Whereas, LEED pattern 300° C grown sample confirms the disappearance of alloy phase from surface and formation of oxide phase. ARPES data also confirms the presence of surface state bands which is essentially a signature of alloy phase for along both $\bar{\Gamma}$ - \bar{K} direction and $\bar{\Gamma}$ - \bar{M} direction. The surface band was not visible for 300° C grown sample and also new bands appears with parabolic dispersion. So, it can be concluded to grow tin oxide by oxidation of Sn-Ag surface alloy 300° C is more appropriate temperature than 250° C.

VI. ACKNOWLEDGEMENTS

I thank Prof. Krishnakumar Menon, Saha Institute of Nuclear Physics for providing LEED and ARPES facility and his valuable inputs.

REFERENCES

- [1] D.P. Woodruff, Ed., The Chemical Physics of Solid Surfaces, (Vol-9, Elsevier 2001).
- [2] P. A. Cox, Transition Metal Oxides. An Introduction to their Electronic Structure and Properties (Oxford: Clarendon, 1992).
- [3] C. R. Ast, J. Henk, A. Ernst, L. Moreschini et al., Phys. Rev. Lett. 98, 2007, 186807.
- [4] L. Moreschini, A. Bendounan, I. Gierzet et al., Phys. Rev. B. 79, 2009, 075424.
- [5] D. Pacile, C. R. Ast, M. Papagno et al., Phys. Rev. B 73, 2006, 245429.
- [6] M. Batzill, U. Diebold, Prog. Surf. Sci. 79, 2005, 47.
- [7] W. K. Choi, H. Sung, K. H. Kim et al., J. Mat. Sci. Lett. 16, 1997, 1551.
- [8] Z. Han, N. Guo, F. Li et al., Materials Letters 48/2, 2001, 99.
- [9] S. Chakraborty, K. S. R. Menon, Vacuum, 160, 2019, 371–377.
- [10] F. Izumi, J. Solid State Chem. 38, 1981, 381.
- [11] L. A. Errico, Physica B, 389, 2007, 140.
- [12] N.E. Christensen, A. Svane, E. L. Peltzer y Blancá, Phys. Rev. B, 72, 2005, 014109.
- [13] A. Bolzan, C. Fong, B. Kennedy et al., Acta Crystallogr. B, 53, 1997, 373.
- [14] R. Hazen, L. Finger, J. Phys. Chem. Solids, 42, 1981, 143.
- [15] G. H. Moh, Chem. Erde, 33, 1974, 243.
- [16] D. J. McPherson and M. Hanson, Trans. ASME, 45, 1953, 915.
- [17] A. Seko, A. Togo, F. Oba et al., Phys. Rev. Lett., 100, 2008, 045702.
- [18] J. Geurts, S. Rau, W. Richter, and F. J. Schmitte, Thin Solid Films, 121, 1984, 217.
- [19] M. S. Moreno, R. C. Mercader, and A. G. Bibiloni, J. Phys. Condens. Matter, 4, 1992, 351.
- [20] M. Batzill, U. Diebold, Prog. Surf. Sci., 79, 2005, 47.
- [21] Y. Ogo, H. Hiramatsu, K. Nomura et al., Appl. Phys. Lett., 93, 2008, 032113.
- [22] K. Suito, N. Kawai, and Y. Masuda, Mater. Res. Bull., 10, 1970, 677.
- [23] L. Lau and G. K. Wertheim, J. Vac. Sci. Technol., 15, 1978, 622.
- [24] V. M. Jimenez, J. A. Mejias, J. P. Espinos et al., Surf. Sci., 366, 1996, 545.
- [25] J. M. Themlin, M. Chtaib, L. Henrard et al., Phys. Rev. B, 46, 1992, 2460.
- [26] S. Chakraborty and K. S. R. Menon, Vacuum, 125, 2016, 106.
- [27] S. Chakraborty and K. S. R. Menon, J. Vac. Sci. Technol., A, 34, 2016, 041513.
- [28] S. Chakraborty and K. S. R. Menon, Growth and structural evolution of Sn on Ag (111) beyond 1/3 monolayer : formation of bulk ($\sqrt{3} \times \sqrt{3}$) R30° structure, communicated.
- [29] J. R. Osiecki and R. I. G. Uhrberg, Phys. Rev. B., 87, 2013, 075441.
- [30] S. K. Mahatha and K. S. R. Menon, Current Science, 98, 2010, 759.